

**FLY ASH STABILIZATION OF RECYCLED ASPHALT
PAVEMENT MATERIAL IN WASECA, MINNESOTA**

by

Lin Li, Craig H. Benson, Tuncer B. Edil, and Bulent Hatipoglu

Geo Engineering Report No. 06-18

Department of Civil and Environmental Engineering
University of Wisconsin-Madison
Madison, Wisconsin 53706
USA

June 9, 2006

EXECUTIVE SUMMARY

This report describes a field site where Class C fly ash was used to stabilize recycled pavement material (RPM) during construction of a flexible pavement in Waseca, MN. The project consisted of pulverizing the existing hot-mix asphalt (HMA), base, and subgrade to a depth of 300 mm to form RPM, blending the RPM with fly ash (10% by dry weight) and water, compacting the RPM, and placement of a new HMA surface. California bearing ratio (CBR), resilient modulus (M_r), and unconfined compression (q_u) tests were conducted on the RPM alone and the fly-ash stabilized RPM (SRPM) prepared in the field and laboratory to evaluate how addition of fly ash improved the strength and stiffness. *In situ* testing was also conducted on the RPM and SRPM with a soil stiffness gauge (SSG), dynamic cone penetrometer (DCP), and falling weight deflectometer (FWD). A pan lysimeter was installed beneath the roadway to monitor the quantity of water percolating from the pavement and the concentration of trace elements in the leachate. A column leaching test was conducted in the laboratory for comparison.

Addition of fly ash improved the stiffness and strength of the RPM significantly. After 7 d of curing, the SRPM prepared in the laboratory using materials sampled during construction had CBR ranging between 70 and 94, M_r between 78 and 119 MPa, and unconfined compressive strengths between 284 and 454 kPa, whereas the RPM alone had CBR between 3 and 17 and M_r between 46 and 50 MPa. Lower CBR, M_r , and q_u were obtained for SRPM mixed in the field relative to the SRPM mixed in the laboratory (64% lower for CBR, 25% lower for M_r , and 50% lower for q_u). Moduli back-calculated from the FWD data were in good agreement with those obtained with the SSG, but were higher than moduli obtained from the M_r tests due to differences in the magnitude of the bulk stress and strain existing *in situ* and applied in the

laboratory. Testing conducted approximately one year after construction showed no degradation in the modulus of the SRPM, even though the SRPM underwent a freeze-thaw cycle.

Percolation from the pavement was seasonally dependent, with peak flows occurring in summer and no flow occurring in winter. Approximately 2 pore volumes of flow (PVF) drained from the lysimeter during the monitoring period. Analysis of leachate collected in the lysimeter showed that concentrations of many trace elements were increasing toward the end of the study, indicating that longer-term monitoring of the lysimeter is needed to characterize the field leaching behavior of the SRPM. In contrast, for the laboratory column test, leachate concentrations peaked within approximately one PVF and then leveled-off or diminished. For leachate collected in the lysimeter, concentrations of all but one element (Mn) were below USEPA maximum contaminant levels (MCLs) and health-risk levels (HRLs) established by the Minnesota Dept. of Public Health (Mn exceeded the HRL). For the column test, these thresholds were exceeded for B (HRL exceeded), Pb (MCL and HRL exceeded), Se (MCL and HRL exceeded), Sr (HRL exceeded), and Mn (HRL exceeded).

This page left blank intentionally.

ACKNOWLEDGEMENT

Financial support for this study was provided by the Minnesota Local Road Research Board (LRRB). The study was administered by the Minnesota Department of Transportation (Mn/Dot). The conclusions and recommendations in this report are solely those of the authors and do not reflect the opinions or policies of LRRB or Mn/DOT. Appreciation is expressed to the City of Waseca's Department of Engineering for supporting the field investigation, providing FWD testing, and for monitoring the lysimeter. Xiaodong Wang, Jacob Sauer, Maria Rosa, and Onur Tastan assisted with the project in the field and laboratory.

This page left blank intentionally.

TABLE OF CONTENTS

EXECUTIVE SUMMARY

ACKNOWLEDGEMENT

1. INTRODUCTION	1
2. MATERIALS.....	3
2.1 Subgrade and RPM	3
2.2 Fly Ash	4
2.3 SRPM	4
3. LABORATORY TEST METHODS	6
3.1 CBR	6
3.2 Resilient Modulus and Unconfined Compression Tests	6
3.3 Column Leaching Test	7
4. FIELD METHODS.....	9
4.1 Environmental Monitoring	9
4.2 Mechanical Evaluation of Pavement Materials	10
5. ENVIRONMENTAL DATA.....	12
5.1 Meteorological and Subsurface Conditions	12
5.2 Trace Elements in Lysimeter Drainage	13
5.3 Trace Elements in CLT Effluent	14
6. PROPERTIES OF SRPM AND RPM	16
6.1 Laboratory Test Data	16
6.2 Field Test Data	18
7. CONCLUSIONS AND RECOMMENDATIONS	21
8. REFERENCES	23
TABLES	25
FIGURES.....	30
APPENDICES	43

This page left blank intentionally.

LIST OF TABLES

- Table 1. Physical properties and classifications of subgrade soils.
- Table 2. Particle size fractions, in situ water content, and compaction characteristics of RPM.
- Table 3. Chemical composition and physical properties of Riverside 7 fly ash and typical Class C and F fly ashes.
- Table 4. CBR, M_r , and q_u of RPM and SRPM.

LIST OF FIGURES

- Fig. 1. Layout of stations along 7th Avenue and 7th Street in Waseca, MN.
- Fig. 2. Particle size distributions of the subgrade (a) and RPM (b).
- Fig. 3. Air and soil temperatures (a) and volumetric water content (b) of the SRPM and subgrade. Air temperature is shown in black. Soil temperature and water content measured at three depths: 150 mm bgs (mid-depth in SRPM) shown in red and designated as T1, 425 mm bgs (subgrade) shown in green and designated as T2, and 675 mm bgs (subgrade) shown in blue and designated as T3.
- Fig. 4. Drainage from the pavement collected in the lysimeter. Base of lysimeter is located at the bottom of the SRPM layer.
- Fig. 5. Concentrations of trace elements in leachate collected in lysimeter: (a) elements with peak concentrations between 3 and 102 $\mu\text{g/L}$ and (b) elements with peak concentrations less than 2.5 $\mu\text{g/L}$.
- Fig. 6. Concentrations of trace elements in effluent from CLT on SRPM: (a) elements with peak concentrations exceeding 100 $\mu\text{g/L}$ and (b) elements with peak concentrations less than 100 $\mu\text{g/L}$.
- Fig. 7. California bearing ratio of RPM and SRPM (laboratory-mix and field-mix) after 7 d of curing.
- Fig. 8. Resilient modulus of RPM and SRPM (laboratory-mix and field-mix) after 14 d of curing.
- Fig. 9. Unconfined compressive strength (q_u) of SRPM (laboratory-mix and field-mix) after 7 d of curing.
- Fig. 10. Dynamic penetration index (DPI) and stiffness of uncompacted RPM and SRPM after compaction and 7 d of curing. DPI was measured with a DCP and stiffness was measured with a SSG.
- Fig. 11. Maximum deflection from the 40-kN drop for FWD tests conducted in November 2004 and August 2005.
- Fig. 12. Modulus of SRPM obtained by inverting FWD data, from SSG measurements, and from resilient modulus tests conducted in the laboratory: (a) modulus along the alignment and (b) box plots of each set of modulus measurements.

This page left blank intentionally.

1. INTRODUCTION

In-place recycling of pavement materials is an attractive method to rehabilitate deteriorated flexible pavements due to lower costs relative to new construction and the long-term societal benefits associated with sustainable construction methods. One approach is to pulverize and blend the existing hot-mix asphalt, base, and some of the subgrade to form a broadly graded granular material referred to as recycled pavement material (RPM) that can be used in place as base course for a new pavement. Blending is typically conducted to a depth of approximately 300 mm and, in cases where the surface elevation is fixed, some of the blended material is removed and used for other applications. The RPM is compacted to form the new base course and is overlain with new hot-mix asphalt (HMA).

The residual asphalt and fines from the underlying subgrade may result in RPM having lower strength and stiffness compared to compacted virgin base material. Thus, methods to enhance the strength and stiffness of RPM are being considered, including the addition of stabilizing agents such as asphaltic oils, cements, and self-cementing coal fly ash (a residue from coal combustion that is normally landfilled). Stabilization is believed to increase the service life of the rehabilitated pavement or permit a thinner HMA layer (Turner, 1997; Croveti, 2000; Mallick et al., 2002; Wen et al., 2003; Robinson et al., 2004). The use of fly ash for stabilization is particularly attractive because fly ashes traditionally have been disposed in landfills. Consequently, using fly ash for stabilization promotes sustainable construction and improves the pavement structure (Edil et al., 2002; Bin-Shafique et al., 2004; Trzebiatowski et al., 2004). However, the effectiveness of stabilizing RPM with coal fly ash is largely undocumented. Providing documentation was a primary objective of this study.

This report describes a project where self-cementing Class C fly ash from a coal-fired electric power plant was used to stabilize a RPM during rehabilitation of a 0.5-km section of flexible pavement along 7th Avenue and 7th Street in Waseca, MN (\approx 125 km south of Minneapolis). RPM was prepared by pulverizing the existing asphalt pavement and underlying materials to a depth of 300 mm below ground surface (bgs) using a CMI RS-650-2 road reclaimer. The uppermost 75 mm of the RPM was removed and then Class C fly ash (10% by dry weight) was spread uniformly on the surface using truck-mounted lay-down equipment similar to that described in Edil et al. (2002). The fly ash was mixed with the RPM to a depth of 150 mm using the road reclaimer, with water being added during mixing using a water truck (see photographs in Appendix A). This mixture, which contained 10% fly ash by dry weight, was compacted within 1-2 h by a tamping foot compactor followed by a vibratory steel drum compactor. The SRPM was cured for 7 d and then overlain with 75 mm of HMA.

2. MATERIALS

2.1 Subgrade and RPM

Disturbed samples of subgrade soil and recycled pavement material (RPM) (≈ 20 kg each) were collected at 10 stations during construction (Fig. 1). Tests were conducted on each sample to determine index properties, soil classification, water content, dry unit weight, compaction characteristics (RPM only), and CBR.

A summary of the properties of the subgrade is shown in Table 1. Particle size distribution curves for the subgrade are shown in Fig. 2. The subgrade consists of highly plastic organic clay (CH) or silt (MH), clayey sand (SC), or silty sand (SM) according to the Unified Soil Classification System. However, coarse silty gravel is present in one region (Station 3). According to the AASHTO Soil Classification System, most of subgrade soils at this site are A-7 with a group index (GI) larger than 20. Two of the coarse-grained subgrade soils classify as A-2-7 (Stations 3 and 8) and have $GI < 2$. CBR of the subgrade soils ranges from 2 to 11 (mean = 5), indicating that the subgrade is soft.

A summary of the properties of the RPM is shown in Table 2 and particle size distribution curves for the RPM are shown in Fig. 2. The blending during production of RPM results in a material that is spatially uniform in particle size distribution, compaction characteristics, and water content. The particle size distribution curves fall in a relatively narrow band (Station 1 excluded) and have the convex shape typically associated with crushed materials that are not post-processed. Most of the RPM consists of sand and gravel-size particles (> 75 μm), which reflects the presence of the pulverized asphalt and the original base course. The *in situ* water content of the RPM was approximately 4% dry of optimum water content based on standard compaction effort (ASTM D 698).

2.2 Fly Ash

Fly ash from Unit 7 of the Riverside Power Station in St Paul, MN was used for stabilization. Chemical composition and physical properties of the fly ash are summarized in Table 3 along with the composition of typical Class C and F fly ashes. The calcium oxide (CaO) content is 24%, the silicon dioxide (SiO₂) content is 32%, the CaO/SiO₂ ratio (indicative of cementing potential, Edil et al., 2006) is 0.75, and the loss on ignition is 0.9%. According to ASTM C 618, Unit 7 fly ash is a Class C fly ash.

2.3 SRPM

Water content and unit weight of the compacted SRPM were measured at each station using a nuclear density gage (ASTM D 2922) immediately after compaction was completed. Grab samples (≈ 20 kg) of SRPM were also collected at these locations and were immediately compacted into a CBR mold (114 mm inside diameter x 152 mm height) and a resilient modulus mold (102 mm inside diameter x 203 mm height) to the unit weight measured with the nuclear density gage. Three lifts were used for the CBR specimens and six lifts were used for the M_r specimens. After compaction, the specimens were sealed in plastic and stored at 100% humidity for curing (7 d for CBR specimens, 14 d for M_r and q_u specimens). These test specimens are referred to henceforth as ‘field-mix’ specimens. Because of the cementing effects of the fly ash, index testing was not conducted on the SRPM.

Undisturbed samples of SRPM were also collected after compaction using thin-wall sampling tubes. These samples were cured at 25 °C and 100% relative humidity for 14 d. However, disturbance incurred during sampling or extrusion rendered the undistributed samples

useless. Similar problems with samples collected with thin-wall tubes have been reported for fly-ash stabilized soils (Edil et al. 2002) and cement-stabilized wastes (Benson et al. 2002).

Specimens of SRPM were also prepared in the laboratory using samples of the RPM and fly ash collected during construction. These specimens, referred to henceforth as 'laboratory-mix' specimens, were prepared with 10% fly ash (dry weight) at the mean field water content (7.9%) and mean dry unit weight (19.1 kN/m^3). The laboratory-mix specimens were compacted and cured using the procedures employed for the field-mix specimens. A similar set of specimens was prepared with RPM only (no fly ash) using the same procedure, except for the curing phase.

3. LABORATORY TEST METHODS

3.1 CBR

The CBR tests were conducted in accordance with ASTM D 1883 after 7 d of curing (field-mix or laboratory-mix SRPM) or immediately after compaction (RPM). The specimens were not soaked and were tested at a strain rate of 1.3 mm/min. The 7-d curing period and the absence of soaking are intended to represent the competency of the RPM when the HMA is placed (Bin-Shafique et al., 2004). Data from the unsoaked CBR tests were not intend as a measure of stiffness of the SRPM and are not for use in pavement design with SRPM.

3.2 Resilient Modulus and Unconfined Compression Tests

Resilient modulus tests on the SRPM and RPM were conducted following the methods described in AASHTO T292 after 14 d of curing (SRPM) immediately after compaction (RPM). The 14-d curing period is based on recommendations in Turner (1997), and is intended to reflect the condition when most of the hydration is complete (Edil et al., 2006). The loading sequence for cohesive soils was used for the SRPM as recommended by Bin-Shafique et al. (2004) and Trzebiatowski et al. (2004) for soil-fly ash mixtures. RPM was tested using the loading sequence for cohesionless soils. Five specimens of field-mix SRPM split horizontally after curing. These specimens were trimmed to an aspect ratio of 1 prior to testing. All other specimens had an aspect ratio of 2.

Unconfined compressive strength was measured on specimens of SRPM after the resilient modulus tests were conducted. Only those specimens having an aspect ratio of 2 were tested. The strains imposed during the resilient modulus test may have reduced the peak

undrained strength of the SRPM. However, strains in a resilient modulus test are small. Thus, the effect on peak strength is believed to be negligible.

A strain rate of 0.21%/min was used for the unconfined compression tests following the recommendations in ASTM D 5102 for compacted soil-lime mixtures. No standard method currently exists for unconfined compression testing of materials stabilized with fly ash, including stabilized RPM.

3.3 Column Leaching Test

A column leaching test (CLT) was conducted on a specimen of field-mix SRPM collected from Station 9. The specimen was prepared in the field in a standard Proctor compaction mold (height = 116 mm, diameter = 102 mm) using the same procedure employed for the specimens of field-mix SRPM prepared for CBR testing. The specimen was cured for 7-d prior to testing.

The CLT was conducted following the procedure described in ASTM D 4874, except a flexible-wall permeameter was used instead of a rigid-wall permeameter. Flow was oriented upward and was driven by a peristaltic pump set to provide a Darcy velocity of 2 mm/d. The effective confining pressure was set at 15 kPa. A 0.1 M LiBr solution was used as the permeant liquid to simulate percolate in regions where salt is used to manage ice and snow (Bin-Shafique et al. 2006). Effluent from the column was collected in sealed Teflon bags to prevent interaction with the atmosphere. Leachate was removed from the bags periodically ($\approx 30 \sim 60$ mL of flow accumulation). Volume of the leachate removed was measured, the pH was recorded, and a sample was prepared for chemical analysis by filtering with a 0.45 μm filter and preservation with nitric acid to $\text{pH} < 2$.

All effluent samples were analyzed by inductively coupled plasma-mass spectrometry (ICP-MS) following the procedure described in USEPA Method 200.8. Analysis was conducted for the following elements (detection limits in $\mu\text{g/L}$ in parentheses): Ag (0.02), As (0.1), B (0.2), Ba (0.02), Be (0.02), Ca (5), Cd (0.08), Co (0.01), Cr (0.04), Cu (0.07), Hg (0.2), Mo (0.08), Mn (0.03), Ni (0.05), Pb (0.01), Sb (0.02), Se (2.0), Sn (0.04), Sr (0.01), Tl (0.006), V (0.06), and Zn (0.2).

4. FIELD METHODS

4.1 Environmental Monitoring

The environmental monitoring program consists of monitoring the volume of water draining from the pavement, concentrations of trace elements in the leachate, temperatures and water contents within the pavement profile, and meteorological conditions (air temperature, humidity, and precipitation). Monitoring of the pavement began in October 2004 and is still being conducted.

Leachate draining from the pavement was monitored using a pan lysimeter installed near the intersection of 7th Street and 7th Avenue (adjacent to Station 9, Fig. 1). The test specimen for the CLT (Section 3.3) was collected near the lysimeter so that a direct comparison could be made between leaching measured in the field and laboratory. The lysimeter is 4 m wide, 4 m long, and 200 mm deep and is lined with 1.5-mm-thick linear low density polyethylene geomembrane. The base of the lysimeter was overlain by a geocomposite drainage layer (geonet sandwiched between two non-woven geotextiles). SRPM was placed in the lysimeter and compacted using the same method employed when compacting SRPM in other portions of the project. Photographs showing the lysimeter are in Appendix B.

Water collected in the drainage layer is directed to a sump plumbed to a 120-L polyethylene collection tank buried adjacent to the roadway. The collection tank is insulated with extruded polystyrene to prevent freezing. Leachate that accumulates in the collection tank is removed periodically with a pump. The volume of leachate removed is recorded with a flow meter, a sample for chemical analysis is collected, and the pH and Eh of the leachate are recorded. The sample is filtered, preserved, and analyzed using the same procedures employed

for the CLT (Section 3.3). Personnel from the City of Waseca collected the samples from the lysimeter.

Air temperature and relative humidity (RH) are measured with a HMP35C temperature/RH probe manufactured by Campbell Scientific Inc. (CSI). A tipping bucket rain gage (CSI TE 525) with snowfall adaptor (CSI CS 705) is used to measure precipitation. Subsurface temperatures and water contents are monitored at three depths: 150 mm below ground surface (bgs) (mid-depth of the SRPM) and 425 and 675 mm bgs (subgrade). Type-T thermocouples are used to monitor temperature and CSI CS616 water content reflectometers (WCRs) are used to monitor volumetric water content. The WCRs were calibrated for the materials on site following the method in Kim and Benson (2002). Data from the meteorological and subsurface sensors are collected with a CSI CR10 datalogger powered by a 12-V deep-cycle battery and a solar panel. Data are downloaded from the datalogger via telephone modem. Photographs of the instrumentation are included in Appendix B.

4.2 Mechanical Evaluation of Pavement Materials

Strength and stiffness of the SRPM were measured with a soil stiffness gauge (SSG), a dynamic cone penetrometer (DCP), a rolling weight deflectometer (RWD), and a falling weight deflectometer (FWD). Photographs of the testing are included in Appendix A. Testing with the SSG, DCP, and RWD was conducted directly on the SRPM after 7 d of curing. FWD testing was conducted two times after the HMA was placed (November 2004 and August 2005). The RWD testing was unsuccessful due to problems with the instrumentation and will not be discussed further.

The SSG tests were conducted in accordance with ASTM D 6758 using a Humboldt GeoGauge. Two measurements were made at each station within a 0.1-m radius. These measurements deviated by less than 10%. Thus, the mean of the two stiffness measurements is reported herein. DCP testing was conducted at each station in accordance with ASTM D 6951 using a DCP manufactured by Kessler Soils Engineering Products Inc. The dynamic penetration index (DPI) obtained from the DCP was computed as the mean penetration (mm per blow) over a depth of 150 mm.

FWD tests were conducted at each station by Braun Intertec Inc. in November 2004 (3 months after construction) and in August 2005 (one year after construction) using a Dynatest™ 8000E FWD following the method described in ASTM D 4694. Moduli were obtained from the FWD deflection data by inversion using MODULUS 5.0 from the Texas Transportation Institute. Analysis of the FWD data was conducted at the University of Wisconsin-Madison.

5. ENVIRONMENTAL DATA

5.1 Meteorological and Subsurface Conditions

Air and soil temperatures between October 2004 and April 2006 are shown in Fig. 3. Data are not shown between April 2005 and May 2005 due to an instrument malfunction. The air temperature ranged from -28 and 32 °C during the monitoring period, with sub-freezing temperatures occurring between October and April each year. Temperature of the SRPM and the subgrade ranged between -12 °C and 32 °C and varied seasonally with the air temperature. The magnitude and frequency of variation diminishes with depth, which reflects the thermal damping provided by the pavement materials.

Frost penetrated to approximately 0.5 m bgs each year, as illustrated by the drop in temperature below 0 °C at depths T1 and T2 and the drops in volumetric water content at T2 when the soil temperature falls below 0 °C (volumetric water contents are not reported in Fig. 3 for periods when freezing was established). These apparent drops in water content reflect freezing of the pore water. The water content measured by WCRs is determined by measuring the velocity of an electromagnetic wave propagated along the probe. The velocity of the wave varies with the apparent dielectric constant of the soil, which is dominated by the dielectric constant of the water phase. When the pore water freezes, the dielectric constant of the water phase drops significantly, which appears as a drop in water content in WCR data (Benson and Bosscher 1999).

Higher water contents were recorded in the fine-textured subgrade than the coarse-grained SRPM, which reflects the greater propensity of fine-textured soils to retain water. No spikes are present in the water content records, which reflects the ability of the HMA to impede infiltration during precipitation and snow melt events and to limit evaporation during drier

periods. The annual variation in water content is also small, with the water content of the SRPM varying between 21 and 26% and the water content of the subgrade varying between 35 and 45%. Higher water contents are recorded in the summer months, when greater precipitation occurs.

The seasonal variation in water content is also reflected in the seasonal variation in drainage collected in the lysimeter, as shown in Fig. 4. The drainage rate varies between 0-1 mm/d throughout the year, with drainage beginning in mid- to late spring (May to June) and the peak drainage rate occurring in mid-summer (July to August). The drainage rate then diminishes to zero by early fall, and remains nil until early spring. On an annual basis, the drainage rate is 0.15 mm/d or 56 mm/yr. A complete summary of the lysimeter data is in Appendix C.

5.2 Trace Elements in Lysimeter Drainage

Approximately 1.8 pore volumes of flow (PVF) have passed through the SRPM during the monitoring period. During this period, pH of the drainage has been near neutral (6.9 – 7.5) and oxidizing conditions have prevailed ($E_h = 48-196$ mV). A summary of the pH and E_h data along with the trace element concentrations is in Appendix C.

Concentrations of trace elements in drainage from the lysimeters are shown in Fig. 5 as a function of PVF. Elements with peak concentrations between 3 and 102 $\mu\text{g/L}$ are shown in Fig. 5a, whereas those with peak concentrations less than 2.5 $\mu\text{g/L}$ are shown in Fig. 5b. Elements not shown in Fig. 5 include those below the detection limit (Be, Ag, Hg, Se, and Tl) and elements not typically associated with health risks (Ca and Mn). All of the concentrations are below USEPA maximum contaminant levels (MCLs) and Minnesota health risk levels (HRLs). The exception is Mn (not shown in Fig. 5), which typically had concentrations between 1 and 2

mg/L. The Minnesota HRL for Mn currently is 100 µg/L, but plans exist to increase the HRL to 1.0-1.3 mg/L (www.pca.state.mn.us). USEPA does not have a MCL for Mn.

Most of the concentrations appear to be increasing, with a more rapid increase towards the end of the monitoring. Thus, higher concentrations are likely to be observed for many of the elements as the lysimeter is monitored in the future. However, concentrations of some elements appear to be decreasing (Mo and Sr) or remaining steady (Sb and Sn). The lack of a steady-state condition or clearly diminished concentrations for most of the trace elements highlights the need for longer term monitoring of the lysimeter.

5.3 Trace Elements in CLT Effluent

Effluent from the CLT had pH between 7.3 and 7.8, which is slightly higher than the pH observed in the leachate from the lysimeter. Concentrations of trace elements in the effluent from the CLT on the SRPM are shown in Fig. 6. Elements having peak concentrations less than 1 µg/L and elements not typically associated with health risks (Ca and Mn) are not shown in Fig. 6. Elements having peak concentrations exceeding 100 µg/L are shown in Fig. 6a, whereas those with peak concentrations less than 100 µg/L are shown in Fig. 6b. A compilation of the data is in Appendix D.

Comparison of Figs. 5 and 6 indicates that the trace element concentrations in the CLT effluent (Fig. 6) typically are higher than concentrations in the drainage collected in the field (Fig. 5). The poor agreement suggests that the CLT test method that was used may not be appropriate for evaluating leaching of trace elements from SRPM, unless a conservative estimate of the trace element concentrations is acceptable. Despite the higher concentrations obtained from the CLT, most of the elements have concentrations below USEPA MCLs and Minnesota

HRLs. The exceptions are for B (peak = 2196 $\mu\text{g/L}$, no MCL, HRL = 600 $\mu\text{g/L}$), Pb (peak = 19 $\mu\text{g/L}$, MCL = 15 $\mu\text{g/L}$, HRL = 15 $\mu\text{g/L}$), Se (peak = 60 $\mu\text{g/L}$, MCL = 50 $\mu\text{g/L}$, HRL = 30 $\mu\text{g/L}$), and Sr (peak = 4023 $\mu\text{g/L}$, no MCL, HRL = 4000 $\mu\text{g/L}$). The peak Mn concentration (468 $\mu\text{g/L}$, not shown in Fig. 6) was also above the current Minnesota HRL for Mn, but is less than the proposed HRL.

The elution behavior observed in the CLT effluent follows two patterns: (i) delayed response, where the concentration initially increases and then falls, and (ii) persistent leaching, where the concentration initially increases and then remains relatively constant. Most of the elements with peak concentrations exceeding 100 $\mu\text{g/L}$ (Fig. 6a) exhibit the persistent leaching pattern (B, Ba, Sr, and Mo), whereas those exhibiting delayed response typically have peak concentrations less than 100 $\mu\text{g/L}$ (Fig. 6b) (Co, Cr, Pb, and Se). The exceptions are Cu and Zn, which have peak concentrations exceeding 100 $\mu\text{g/L}$ and exhibited a delayed response, and As and V, which have peak concentrations less than 100 $\mu\text{g/L}$ and exhibit the persistent leaching pattern.

6. PROPERTIES OF SRPM AND RPM

6.1 Laboratory Test Data

CBR, M_r , and q_u of the SRPM and RPM are summarized in Table 4. Tests were conducted on RPM and laboratory-mix SRPM using samples of RPM from Stations 1, 4 and 7. Samples from these stations were selected to bracket the range of gradation of the RPM (Stations 1 and 7) and to represent typical RPM (Station 4) (see Fig. 2). Tests were conducted on both RPM and SRPM to determine the benefits of adding fly ash to the mixture in terms of strength and stiffness.

CBR of the RPM and SRPM along the alignment of the project is shown in Fig. 7. Stations 1-8 correspond to locations along 7th Avenue and Stations 9 and 10 are along 7th Street (Fig. 1). There is no systematic variation in CBR of the RPM or SRPM along the alignment, suggesting that the variability in the CBR is more likely due to heterogeneity in the material rather than systematic variation in site conditions or construction methods. CBR of the RPM ranges from 3 to 17 (mean = 9), the laboratory-mix SRPM has CBR between 70 and 94 (mean = 84), and the field-mix SRPM has CBR between 13 and 53 (mean = 29). Thus, adding fly ash to the RPM increased the CBR appreciably, although the CBR in the field was 66% lower, on average, than the CBR of the laboratory-mix SRPM. The CBR of the field-mix SRPM also was more variable than the CBR of the laboratory-mix SRPM.

A similar difference between CBRs of mixtures prepared with fly ash in the laboratory and field is reported in Bin-Shafique et al. (2004) for fine-grained subgrade soils. They report that field mixtures of silty clay and Class C fly ash typically have a CBR that is one-third of the CBR of comparable mixtures prepared in the laboratory. Bin-Shafique et al. (2004) attribute

these differences in CBR to more thorough blending of soil and fly ash in the laboratory compared to the field, resulting in more uniform distribution of cements within the mixture.

Resilient moduli of RPM, field-mixed SRPM, and lab-mixed SRPM are shown in Fig. 8 and are summarized in Table 4. These M_r correspond to a deviator stress of 21 kPa, which represents typical conditions within the base course of a pavement structure (Tanyu et al. 2003, Trzebiatowski et al. 2004). Complete M_r curves are included in Appendix E. As observed for CBR, there is no systematic variation in M_r along the alignment. Comparison of the M_r for RPM and SRPM in Fig. 8 and Table 4 indicates that adding fly ash increased the M_r . For the RPM, the M_r ranges between 45 and 50 MPa (mean = 47 MPa), whereas the field-mix SRPM had M_r between 50 and 111 MPa (mean = 78 MPa) and the laboratory-mix SRPM had M_r ranging between 78 and 119 (mean = 104 MPa). As with CBR, M_r of the field-mix SRPM is lower (25%, on average) and more variable than the M_r of the laboratory-mix SRPM.

Unconfined compressive strengths are shown in Fig. 9 and Table 4 for the field-mix and laboratory-mix SRPM. Strengths are not reported for RPM because the RPM is essentially non-cohesive and therefore is not amenable to q_u testing. Data are missing at some of the stations for the field-mix SRPM because the specimens had an aspect ratio less than 2 and could not be tested to determine q_u . As with CBR and M_r , there is no systematic variation in q_u along the alignment. In addition, q_u of the field-mix SRPM is less than one-half of the q_u of the laboratory-mix SRPM, on average. Bin-Shafique et al. (2004) also found that q_u of their field-mix specimens ranged between one-half and two-thirds of the q_u of laboratory-mix specimens.

6.2 Field Test Data

In situ stiffness measured with the SSG and dynamic penetration index (DPI) measured with the DCP are shown in Fig. 10 for the RPM and the SRPM after 7 d of curing. Addition of the fly ash and compaction increased the strength and stiffness appreciably, with the DPI decreasing from 17 to 12 mm/blow, on average, and the stiffness increasing from 6 to 17 MN/m, on average. The DPI and stiffness of the SRPM are also less variable than those of the RPM.

Maximum deflections from the FWD tests for the 40-kN drop are shown in Fig. 11. Maximum deflection, which is measured at the center of the loading plate, is a gross indicator of pavement response to dynamic load. FWD tests were conducted in November 2004 and August 2005 to define the as-built condition and the condition after one year of winter weather. Similar deflections were measured during both surveys, suggesting that the SRPM had maintained its integrity even after exposure to freezing and thawing. The deflection at Stations 4-10 is slightly higher in 2005 than 2004. However, this difference is not caused by a decrease in modulus of the SRPM, as shown subsequently. A more likely cause is the higher temperature of the HMA in August relative to November.

Elastic moduli of the SRPM that were obtained by inversion of the FWD data are shown in Fig. 12a. For the inversion, a three-layer profile was assumed that consisted of asphalt (75-mm thick), SRPM (150-mm thick), and an infinitely thick subgrade. Modulus of the asphalt was allowed to vary between 345 and 11,750 MPa and the Poisson's ratio was set as 0.4. The SRPM was assumed to have a Poisson's ratio of 0.35 and the modulus was allowed to vary between 70-9400 MPa. The subgrade was assumed to have a Poisson's ratio of 0.35.

The modulus of the SRPM varies between 57 and 1248 MPa (mean = 262 MPa) in November 2004 and between 79 and 1379 MPa (mean = 252 kPa) in August 2005. Most of the

moduli are less than 200 MPa. The most significant exception is the very high modulus at Station 3. This modulus is believed to be an anomaly caused by the coarse gravel subgrade near Station 3 (Fig. 2), which was not included in the inversion.

Comparison of the moduli in November 2004 and August 2005 in Fig. 12a suggests that the SRPM was not affected by exposure to freezing and thawing. The close agreement between the mean moduli in November 2004 and August 2005 (262 vs. 252 MPa) also suggests that freeze-thaw cycling did not affect the SRPM. To test this assertion, the data from 2004 and 2005 were compared with a t-test at a significance level of 0.05. The t-test yielded a t-statistic of 0.060 and p of 0.952, confirming that the moduli measured in November 2004 and August 2005 are not statistically different (i.e., $p = 0.952 \gg 0.05$).

Moduli obtained from the FWD inversion are compared with those obtained from the resilient modulus tests on field-mix specimens and the moduli computed from the stiffness measured with the SSG in Fig. 12b. Elastic modulus (E) was computed from the SSG stiffness (K_{SSG}) using (Sawangsurriya et al., 2003):

$$E = \frac{K_{SSG}(1-\nu^2)}{1.77 R} \quad (1)$$

where R is the outside radius of the SSG foot (0.057 m) and ν is Poisson's ratio (assumed to be 0.35). Moduli obtained from the SSG and the FWD are comparable, whereas those from the resilient modulus tests are approximately one-half of those from the SSG and the FWD. Tanyu et al. (2003) and Trzebiatowski et al. (2004) report similar differences between moduli measured determined with FWD, SSG, and resilient modulus test, and attribute the differences in the

moduli to differences in the strain imposed in each test (shear strain $\approx 0.07\%$ for SSG and FWD vs. $0.07\% \sim 0.15\%$ for M_r , Sawangsuriya et al., 2003).

7. CONCLUSIONS AND RECOMMENDATIONS

A case history has been described where Class C fly ash (10% by weight) was used to stabilize recycled pavement material (RPM) during construction of a flexible pavement. California bearing ratio (CBR), resilient modulus (M_r), and unconfined compression (q_u) tests were conducted on the RPM alone and fly-ash stabilized RPM (SRPM) mixed in the field and laboratory to evaluate how addition of fly ash improved the strength and stiffness. *In situ* testing was also conducted on the RPM and SRPM with a soil stiffness gauge (SSG), dynamic cone penetrometer (DCP), and falling weight deflectometer (FWD). A pan lysimeter was installed beneath the pavement to monitor the rate of drainage and trace element concentrations in the leachate. A column leaching test was also conducted on a sample of SRPM collected during construction.

SRPM mixed in the laboratory using materials sampled during construction had significantly higher CBR, M_r , and unconfined compressive strength than RPM that was not stabilized with fly ash. This finding suggests that fly ash stabilization of RPM should be beneficial in terms of increasing pavement capacity and service life. However, the CBR, M_r , and unconfined compressive strength for SRPM mixed in the field were lower than those for SRPM mixed in the laboratory (64% lower for CBR, 25% lower for M_r , and 50% lower for q_u). Similar biases between mixtures prepared in the laboratory and field has been observed by others. Given that mixtures prepared in the laboratory are likely to be used for materials characterization for design, additional study is needed to determine how this bias should be considered in design calculations and how the bias may affect pavement performance in the long term.

Moduli back-calculated from the FWD data were in good agreement with those obtained with the SSG, but were higher than moduli obtained from the M_r tests due to differences in the

magnitude of the bulk stress and strain existing in situ and applied in the laboratory. More importantly, analysis of FWD data collected after a freeze-thaw cycle showed no degradation in the modulus. Nevertheless, longer-term monitoring is needed to confirm that the modulus of SRPM will persist after multiple winter seasons.

Percolation from the pavement occurred only in late spring, summer, and early fall with an average drainage rate of 56 mm/yr. Chemical analysis of the draining leachate showed that equilibrium was not established, with the concentrations of many trace elements increasing toward the end of the study. Thus, longer-term monitoring is needed to fully understand the potential for SRPM to leach trace elements during the service life of a pavement. However, during the monitoring period, none of the trace elements normally associated with health risks exceeded USEPA maximum contaminant levels (MCLs) or health-risk levels (HRLs) established by the Minnesota Dept. of Public Health. Additional study is also needed to define laboratory leach testing protocols that can more accurately simulate leaching of trace elements from SRPM.

8. REFERENCES

- Benson, C.H. (2002), Containment systems: Lessons learned from North American failures, *Environmental Geotechnics* (4th ICEG), Swets and Zeitlinger, Lisse, pp. 1095-1112.
- Benson, C.H. and Bosscher, P.J., 1999. Time-domain reflectometry in geotechnics: a review. In: W. Marr and C. Fairhurst (Editors), *Nondestructive and Automated Testing for Soil and Rock Properties*, ASTM STP 1350. ASTM International, West Conshohocken, PA, pp. 113-136.
- Bin-Shafique, S., Benson, C.H., Edil, T.B. and Hwang, K., 2006. Leachate concentrations from water leach and column leach tests on fly-ash stabilized soils. *Environmental Engineering* 23(1), pp. 51-65.
- Bin-Shafique, S., Edil, T.B., Benson, C.H. and Senol, A., 2004. Incorporating a fly-ash stabilised layer into pavement design. *Geotechnical Engineering*, Institution of Civil Engineers, United Kingdom, 157(GE4), pp. 239-249.
- Crovetti, J.A., 2000. Construction and performance of fly ash-stabilized cold in-place recycled asphalt pavement in Wisconsin, *Issues in Pavement Design and Rehabilitation*. Transportation Research Record, pp. 161-166.
- Edil, T.B., Acosta, H.A. and Benson, C.H., 2006. Stabilizing soft fine-grained soils with fly ash. *Journal of Materials in Civil Engineering*, 18(2), pp. 283-294.
- Edil, T.B. et al., 2002. Field evaluation of construction alternatives for roadways over soft subgrade. *Transportation Research Record*, No. 1786: National Research Council, Washington DC, pp. 36-48.
- FHWA, 2003. *Fly Ash Facts for Highway Engineers*. Federal Highway Administration, US Department of Transportation, Washington D.C., FHWA-IF-03-019.
- Kim, K. and Benson, C.H. (2002), Water content calibrations for final cover soils, *Geo Engineering Report 02-12*, Geo Engineering Program, University of Wisconsin-Madison.
- Mallick, R.B. et al., 2002. Evaluation of performance of full-depth reclamation mixes, *Design and Rehabilitation of Pavements 2002*. Transportation Research Record, pp. 199-208.
- Robinson, G.R., Menzie, W.D. and Hyun, H., 2004. Recycling of construction debris as aggregate in the Mid-Atlantic Region, USA. *Resource Conservation and Recycling*, 42(3), pp. 275-294.
- Sawangsurriya, A., Edil, T.B. and Bosscher, P.J., 2003. Relationship between soil stiffness gauge modulus and other test moduli for granular soils. *Transportation Research Record*, No. 1849: National Research Council, Washington D.C., pp. 3-10.

- Tanyu, B., Kim, W., Edil, T., and Benson, C., 2003. Comparison of laboratory resilient modulus with back-calculated elastic modulus from large-scale model experiments and FWD tests on granular materials. Resilient Modular Testing for Pavement Components, American Society for Testing and Materials, West Conshohocken, PA. STP 1437, pp. 191-208.
- Trzebiatowski, B., Edil, T.B. and Benson, C.H., 2004. Case study of subgrade stabilization using fly ash: State Highway 32, Port Washington, Wisconsin. In: A. Aydilek and J. Wartman (Editors), Beneficial Reuse of Waste Materials in Geotechnical and Transportation Applications, GSP No. 127. ASCE, Reston, VA, pp. 123-136.
- Turner, J.P., 1997. Evaluation of western coal fly ashes for stabilization of low-volume roads, Testing Soil Mixed with Waste or Recycled Materials. American Society for Testing and Materials, West Conshohocken, PA. STP 1275, pp. 157-171.
- Wen, H.F., Tharaniyil, M.P. and Ramme, B., 2003. Investigation of performance of asphalt pavement with fly-ash stabilized cold in-place recycled base course, Eighth International Conference on Low-Volume Roads 2003, Vol. 1 and 2. Transportation Research Record, pp. A27-A31.

TABLES

Table 1. Physical properties and classifications of subgrade soils.

Station	LL	PI	% Fines	GI	LOI (%)	Classification		CBR	w _N (%)	γ _d (kN/m ³)
						USCS	AASHTO			
1	61	41	72.2	29	2.1	CH	A-7	4	21.6	15.5
2	55	27	47.1	9	3.0	SC	A-7	11	13.6	18.2
3	69	30	8.5	0	13.0	GM	A-2-7	-	14.7	18.9
4	57	21	46.7	7	8.8	SM	A-7	2	25.8	14.6
5	122	53	70.2	45	18.3	MH	A-7	-	20.9	13.8
6	77	46	66.4	30	11.1	CH	A-7	5	26.8	14.9
7	69	49	73.8	36	3.4	CH	A-7	3	24.0	15.8
8	68	39	21.1	2	7.3	SC	A-2-7	2	25.7	15.4
9	62	35	67.9	23	3.2	CH	A-7	5	17.2	15.9
10	61	34	67.3	23	-	CH	A-7	-	50.1	12.0

Notes: LL = liquid limit, PI = Plasticity Index, % Fines = percentage passing No. 200 sieve, GI = group index, LOI = loss on ignition, USCS = Unified Soil Classification System, AASHTO = American Association of State Highway and Transportation Officials, CBR = California bearing ratio, w_N = in situ water content, γ_d = in situ dry unit weight, hyphen indicates test was not conducted.

Table 2. Particle size fractions, in situ water content, and compaction characteristics of RPM.

Station	% Gravel	% Sand	% Fines	w _N (%)	w _{opt} (%)	γ _{dmax} (kN/m ³)
1	14.5	69.1	16.4	7.1	11.6	19.6
2	33.6	54.0	12.4	6.6	-	-
3	41.1	55.6	3.3	6.7	-	-
4	33.3	58.0	8.7	7.6	12.0	19.6
5	23.8	65.1	11.1	6.5	-	-
6	40.7	53.1	6.3	6.8	-	-
7	46.7	47.9	5.4	7.3	11.2	20.1
8	30.1	62.6	7.3	ND	-	-
9	35.4	55.9	8.7	8.6	-	-
10	30.0	60.4	9.6	10.3	-	-

Notes: w_N = in situ water content, γ_d = in situ dry unit weight, w_{opt} = optimum water content, γ_{dmax} = maximum dry unit weight, hyphen indicates test was not conducted.

Table 3. Chemical composition and physical properties of Riverside 7 fly ash and typical Class C and F fly ashes.

Parameter	Percent of Composition		
	Riverside 7 ⁺	Typical Class C*	Typical Class F*
SiO ₂ (silicon dioxide), %	32	40	55
Al ₂ O ₃ (aluminum oxide), %	19	17	26
Fe ₂ O ₃ (iron oxide), %	6	6	7
SiO ₂ + Al ₂ O ₃ + Fe ₂ O ₃ , %	57	63	88
CaO (calcium oxide), %	24	24	9
MgO (magnesium oxide), %	6	2	2
SO ₃ (sulfur trioxide), %	2	3	1
CaO/SiO ₂	0.75	-	-
CaO/(SiO ₂ +Al ₂ O ₃)	0.47	-	-
Loss on Ignition, %	0.9	6	6
Moisture Content, %	0.17	-	-
Specific Gravity	2.71	-	-
Fineness, amount retained on #325 sieve, %	12.4	-	-

⁺provided by Lafarge North America, *from FHWA (2003).

Table 4. CBR, M_r , and q_u of RPM and SRPM.

Station	CBR			M_r (MPa)			q_u (kPa)	
	RPM	Field-Mix SRPM	Lab-Mix SRPM	RPM	Field-Mix SRPM	Lab-Mix SRPM	Field-Mix SRPM	Lab-Mix SRPM
1	17	28	70	50	57	NA	-	284
2	-	13	-	-	84	-	185	-
3	-	38	-	-	63	-	-	-
4	3	24	88	45	100	78	198	430
5	-	42	-	-	75	-	134	-
6	-	37	-	-	91	-	158	-
7	7	25	94	46	83	116	144	454
8	-	53	-	-	67	-	-	-
9	-	10	-	-	111	-	-	-
10	-	20	-	-	50	119	-	-

Notes: CBR = California bearing ratio, M_r = resilient modulus, q_u = unconfined compressive strength, hyphen indicates test not conducted, NA = not available because specimen damaged.

FIGURES



Fig. 1. Layout of stations along 7th Avenue and 7th Street in Waseca, MN.

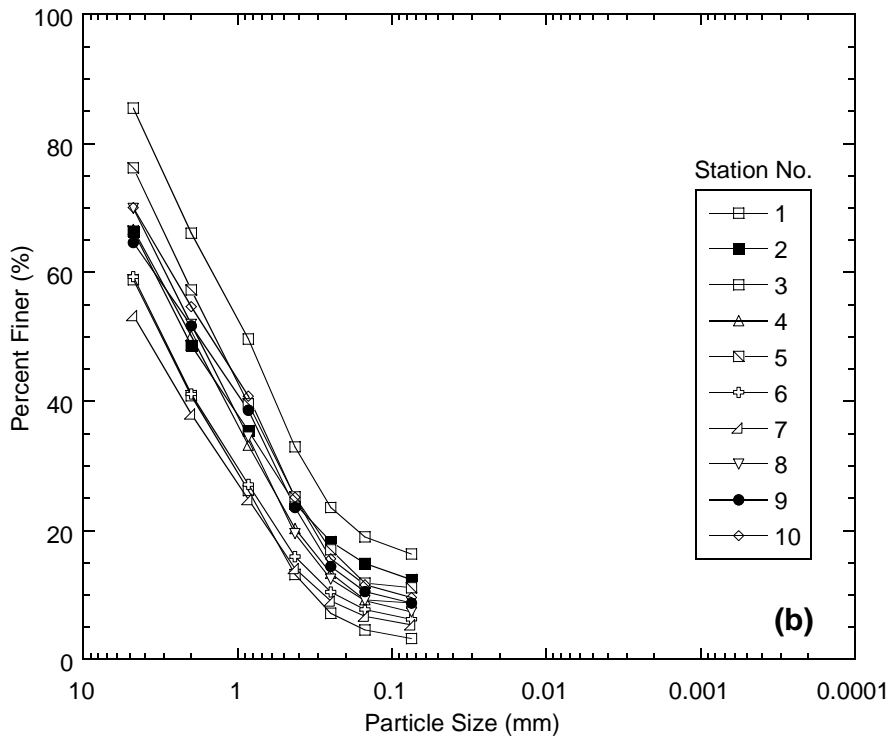
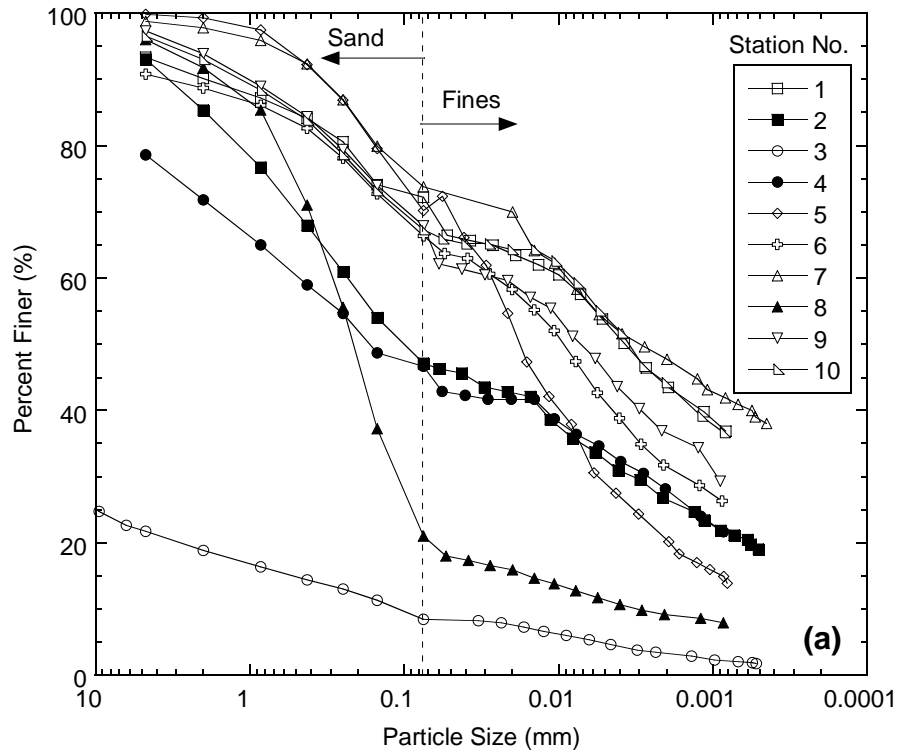


Fig. 2. Particle size distributions of the subgrade (a) and RPM (b).

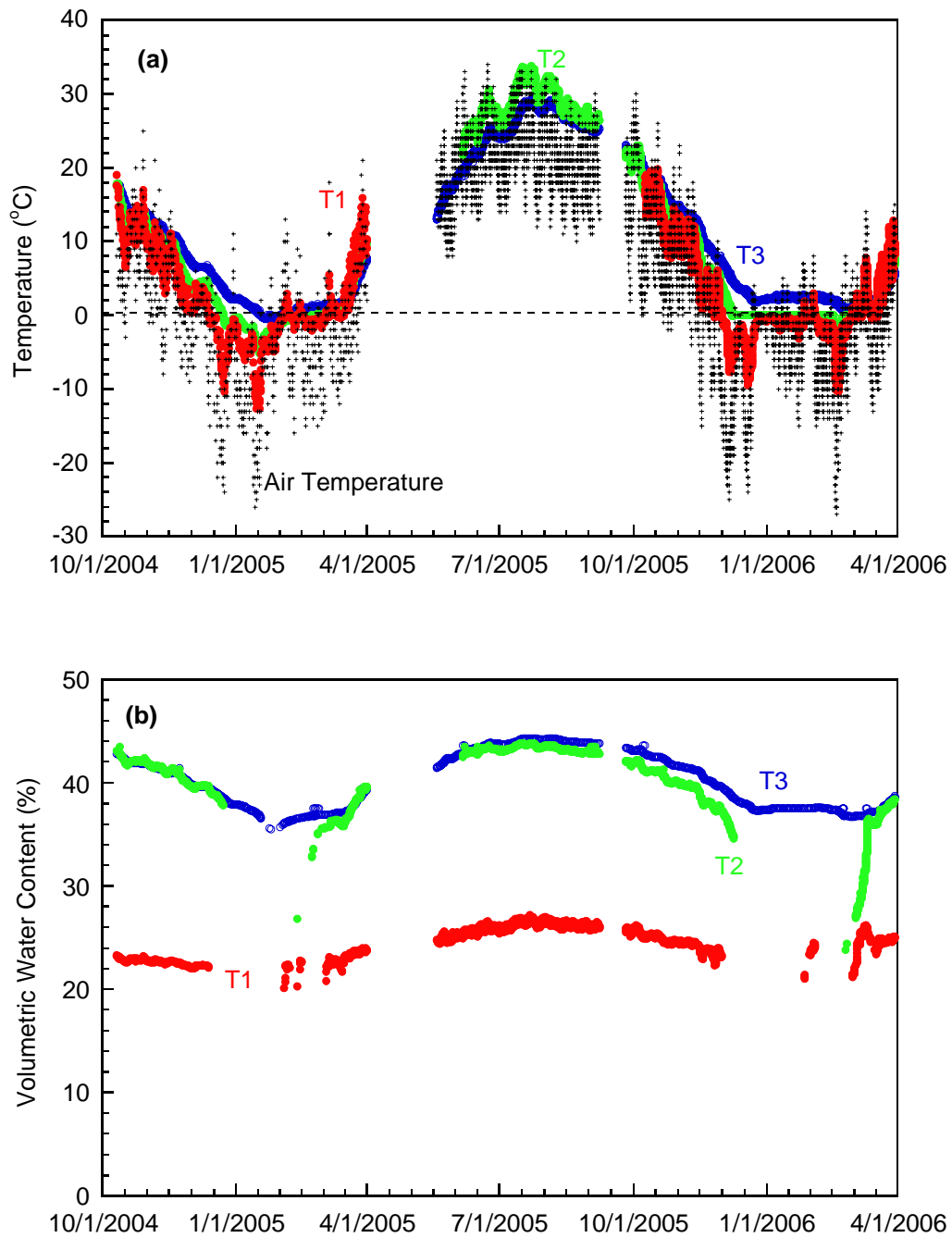


Fig. 3. Air and soil temperatures (a) and volumetric water content (b) of the SRPM and subgrade. Air temperature is shown in black. Soil temperature and water content measured at three depths: 150 mm bgs (mid-depth in SRPM) shown in red and designated as T1, 425 mm bgs (subgrade) shown in green and designated as T2, and 675 mm bgs (subgrade) shown in blue and designated as T3.

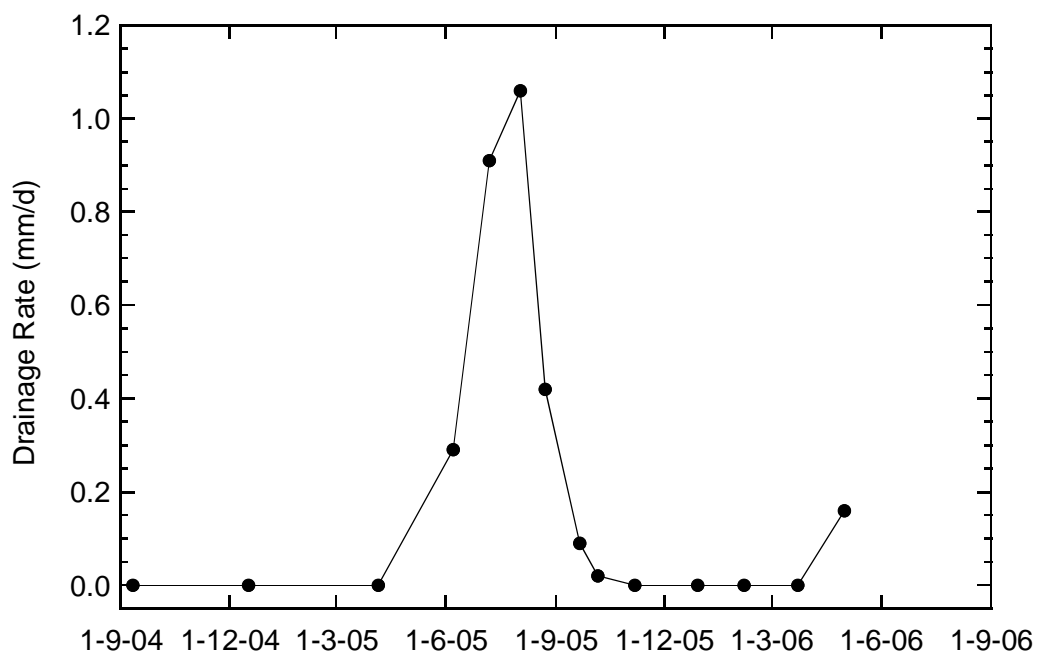


Fig. 4. Drainage from the pavement collected in the lysimeter. Base of lysimeter is located at the bottom of the SRPM layer.

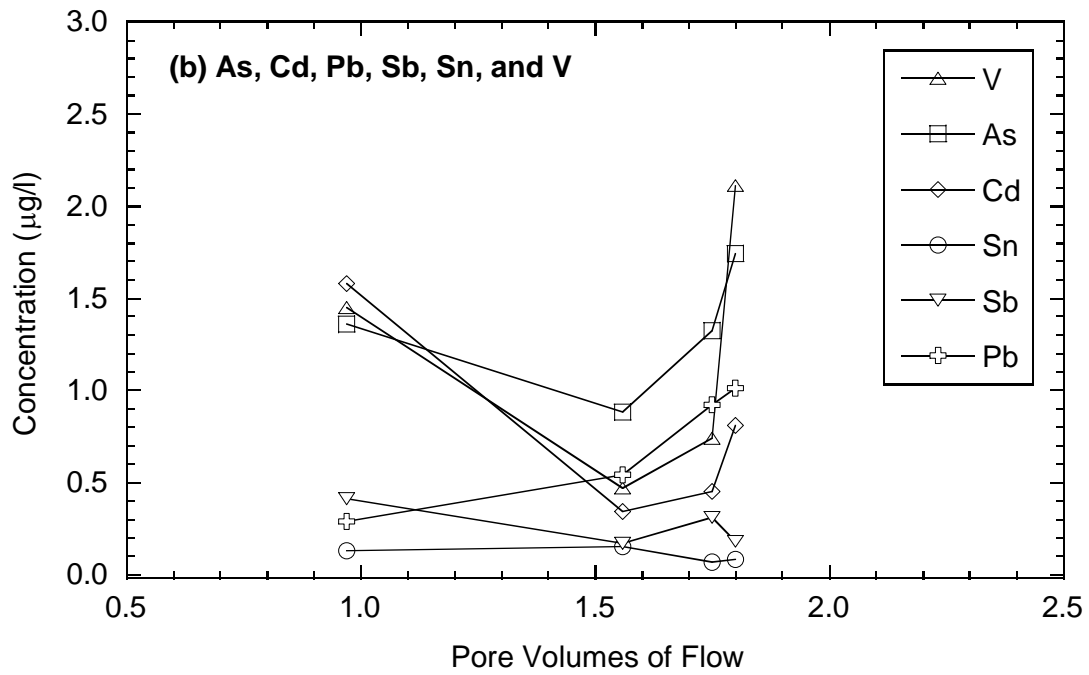
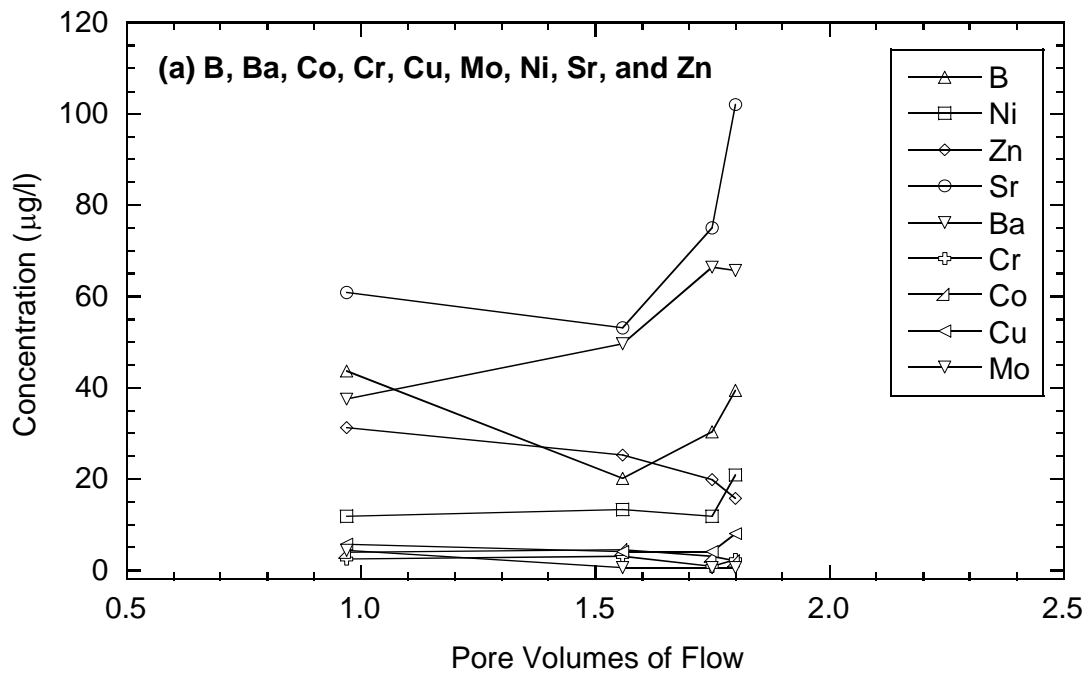


Fig. 5. Concentrations of trace elements in leachate collected in lysimeter: (a) elements with peak concentrations between 3 and 102 $\mu\text{g/L}$ and (b) elements with peak concentrations less than 2.5 $\mu\text{g/L}$.

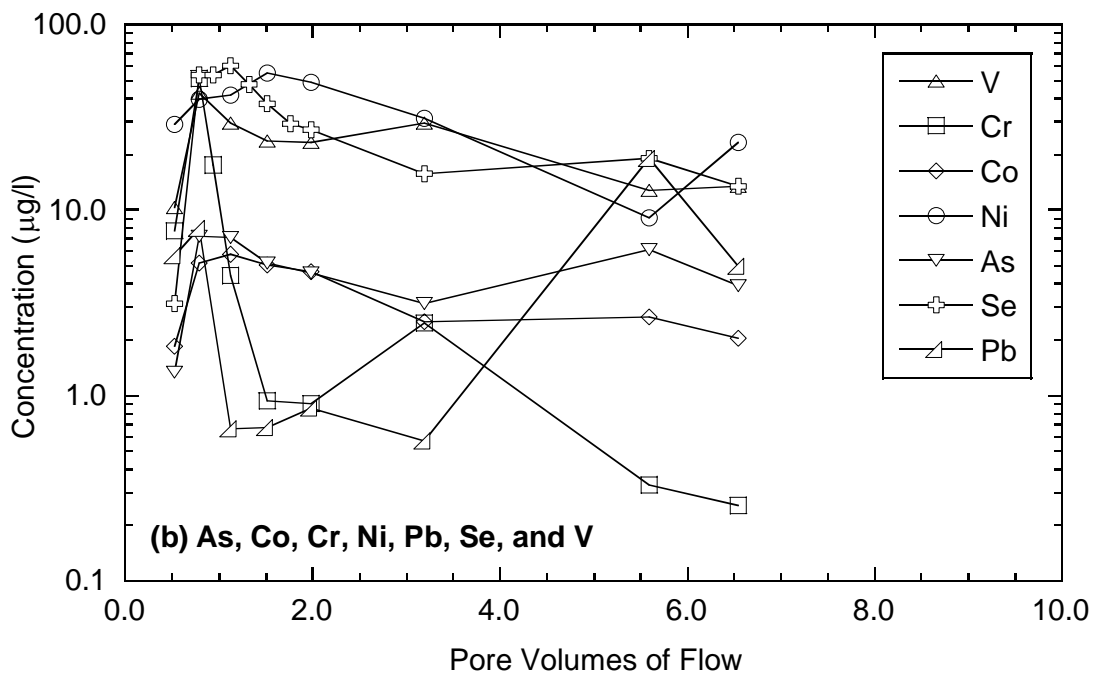
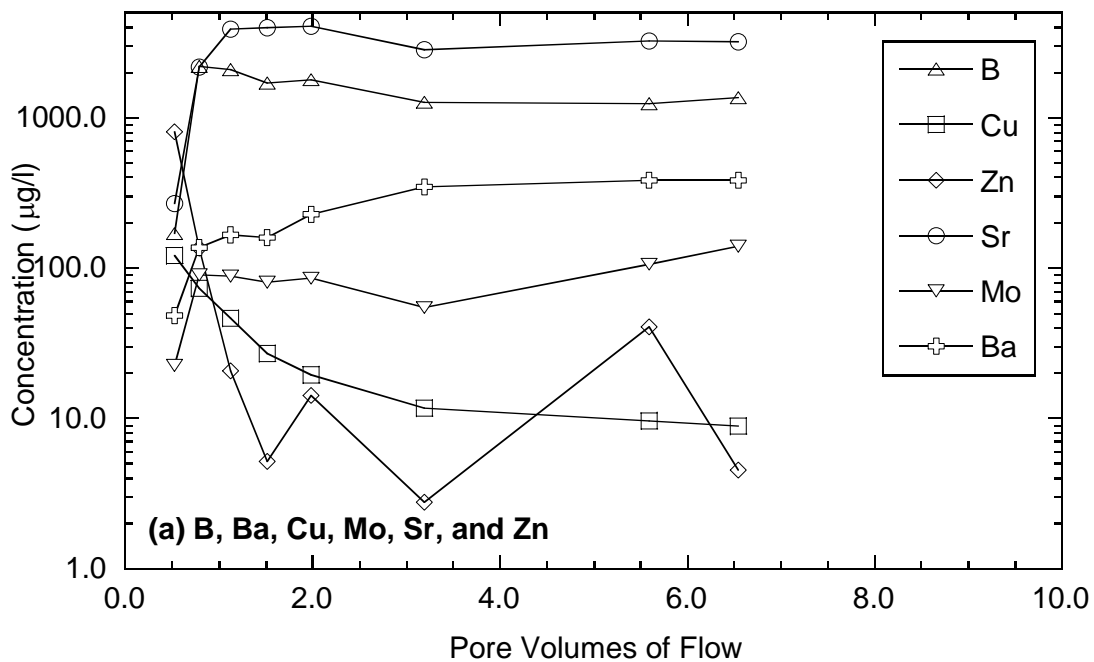


Fig. 6. Concentrations of trace elements in effluent from CLT on SRPM: (a) elements with peak concentrations exceeding 100 µg/L and (b) elements with peak concentrations less than 100 µg/L.

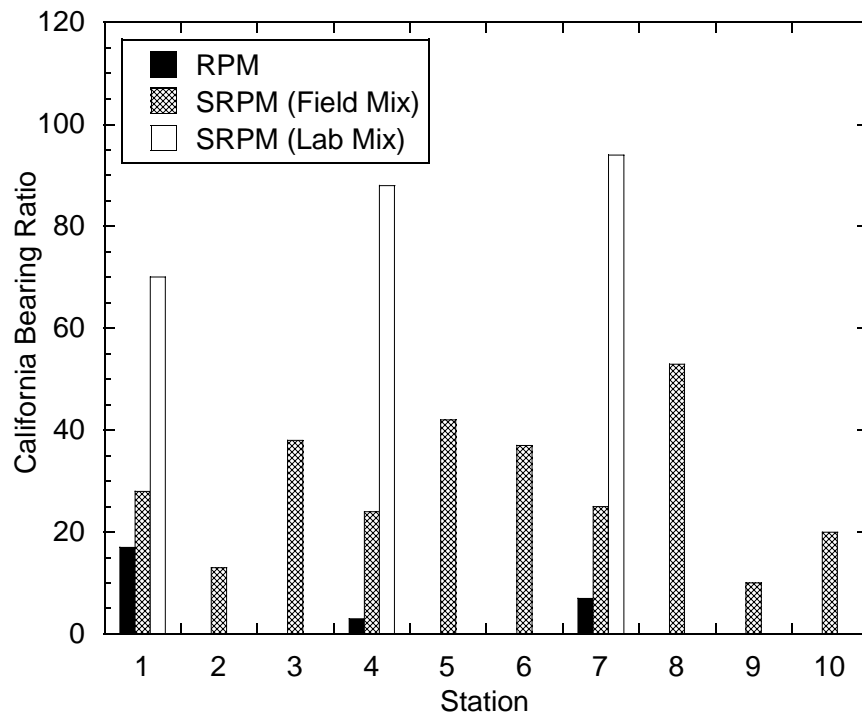


Fig. 7. California bearing ratio of RPM and SRPM (laboratory-mix and field-mix) after 7 d of curing.

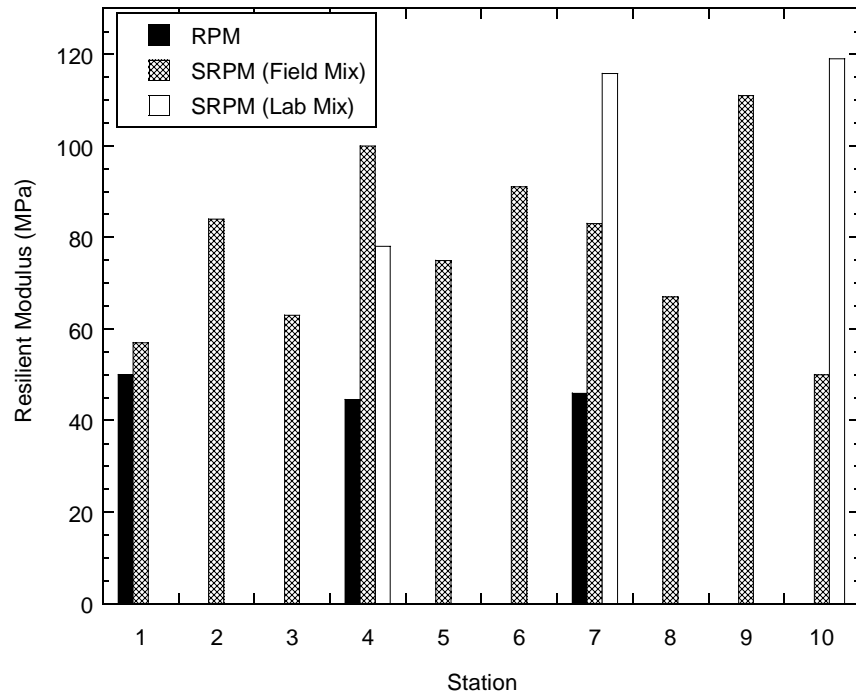


Fig. 8. Resilient modulus of RPM and SRPM (laboratory-mix and field-mix) after 14 d of curing.

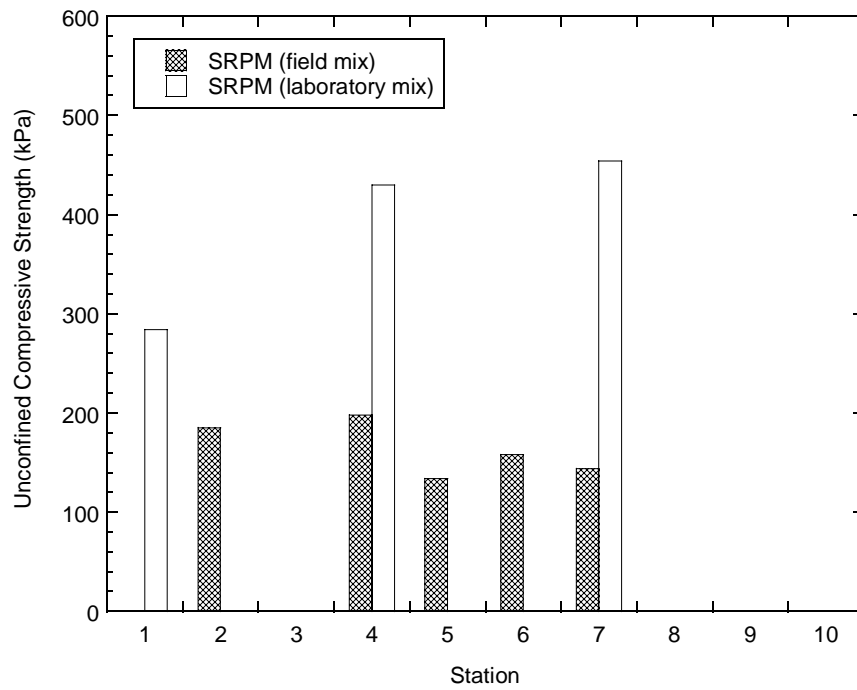


Fig. 9. Unconfined compressive strength (q_u) of SRPM (laboratory-mix and field-mix) after 7 d of curing.

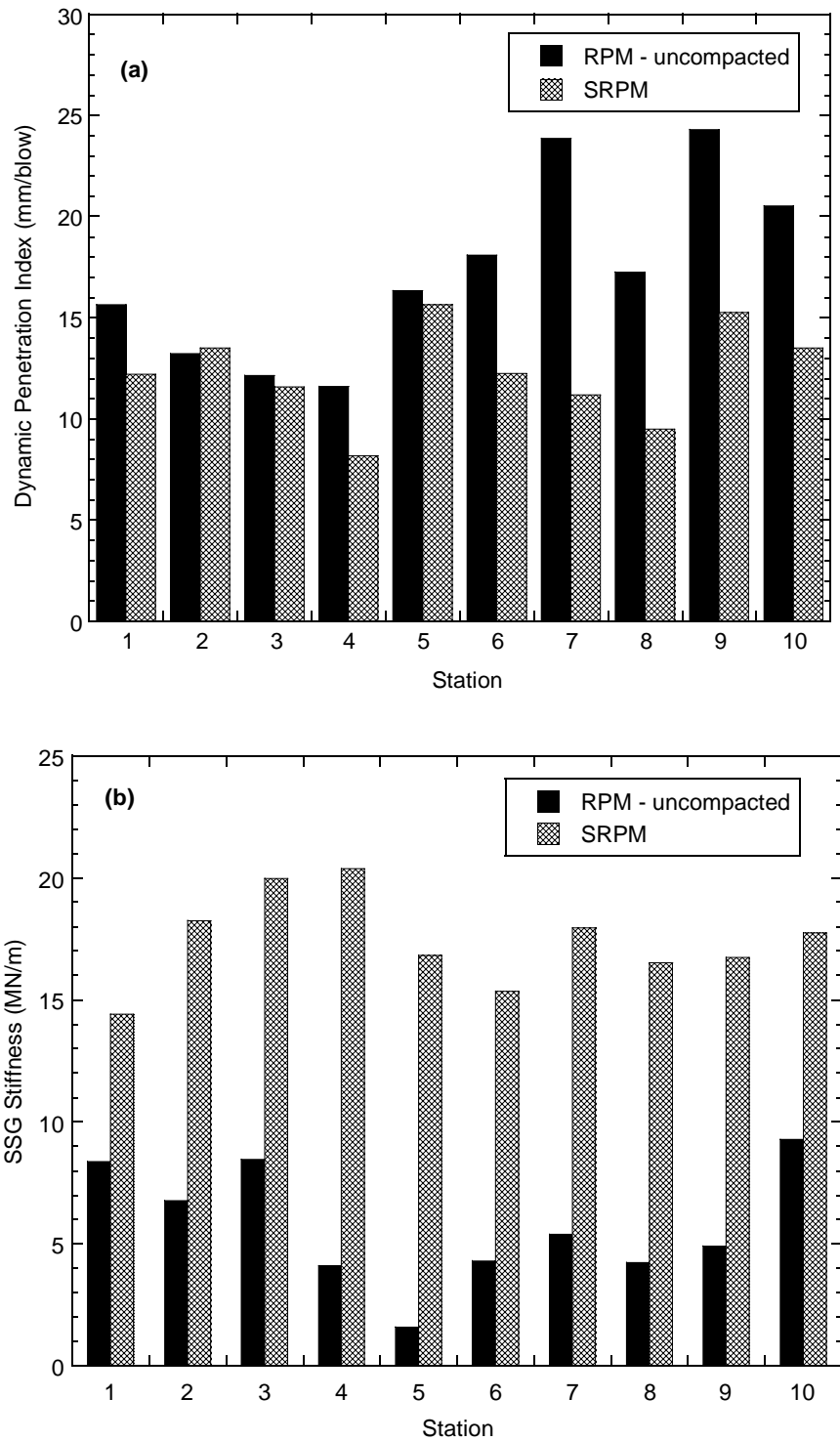


Fig. 10. Dynamic penetration index (DPI) and stiffness of uncompactd RPM and SRPM after compaction and 7 d of curing. DPI was measured with a DCP and stiffness was measured with a SSG.

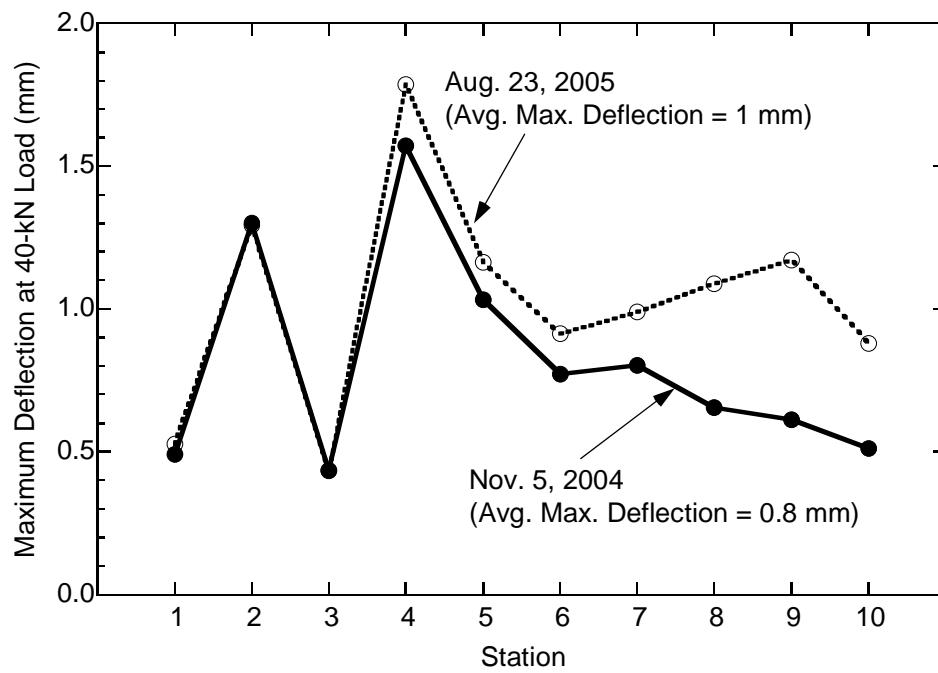


Fig. 11. Maximum deflection from the 40-kN drop for FWD tests conducted in November 2004 and August 2005.

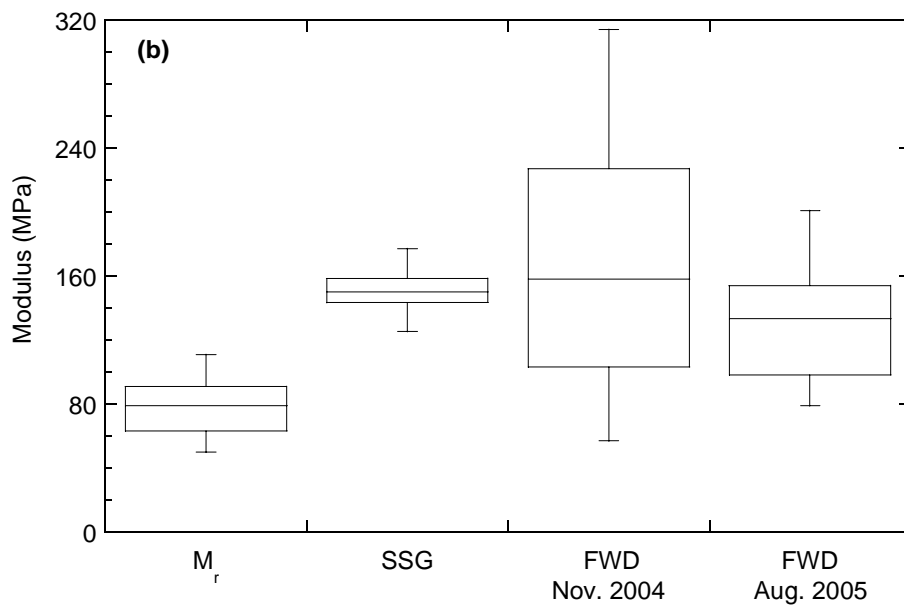
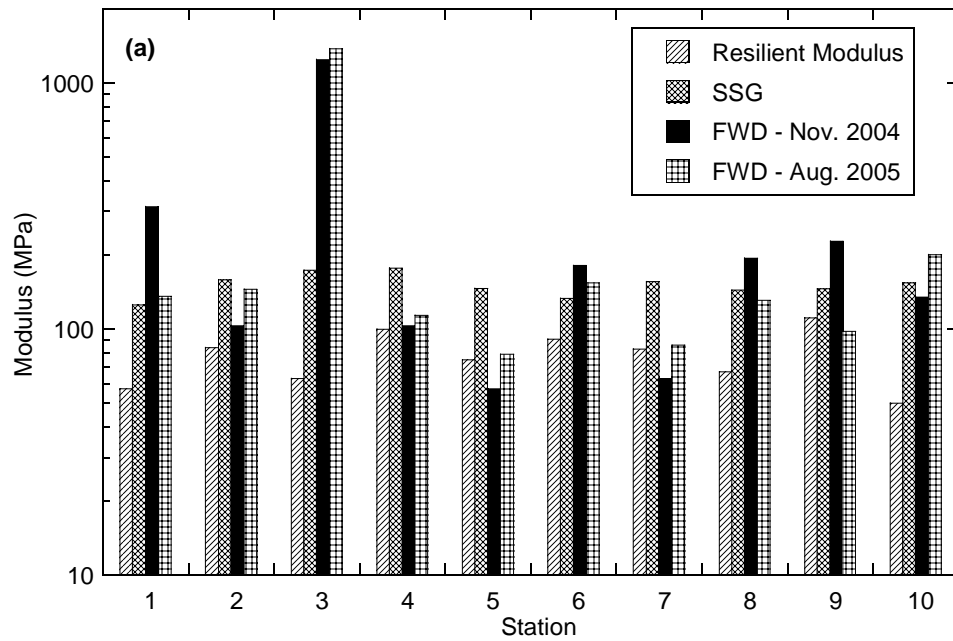


Fig. 12. Modulus of SRPM obtained by inverting FWD data, from SSG measurements, and from resilient modulus tests conducted in the laboratory: (a) modulus along the alignment and (b) box plots of each set of modulus measurements.

APPENDICES

APPENDIX A

CONSTRUCTION PHOTOGRAPHS



Fig. A1. RPM before placement of fly ash.



Fig. A2 Lay-down truck placing fly ash on SRPM.



Fig. A3. Water truck and road-reclaimer blending fly ash, water, and RPM.

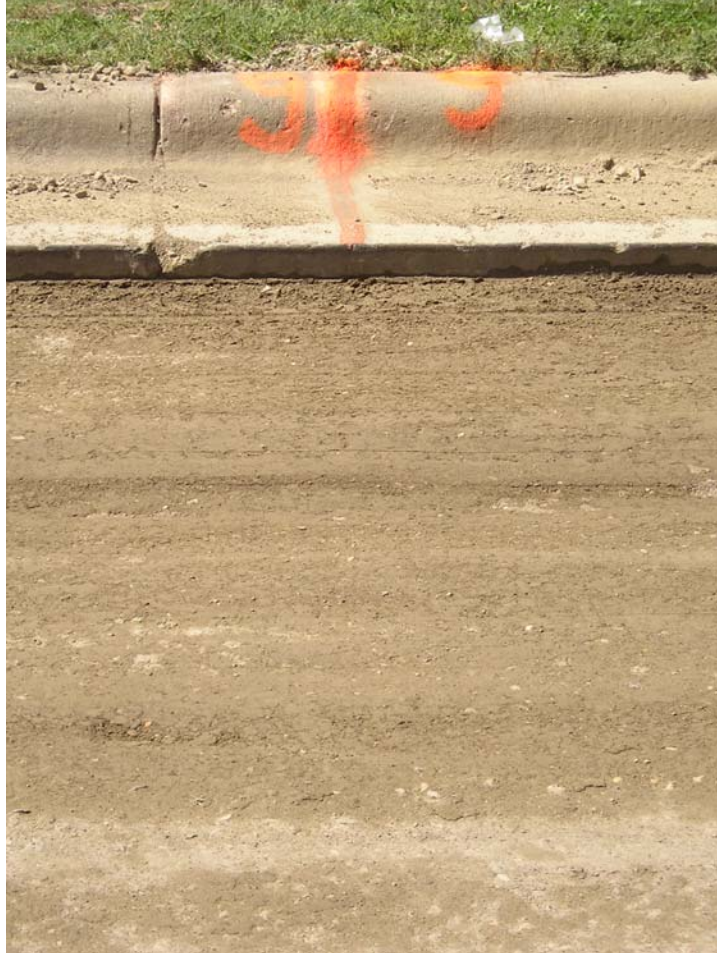


Fig. A4. Surface of SRPM after compaction.



Fig. A5. Mid-section of road-reclaimer showing tines used to blend fly ash, water, and RPM.



Fig. A6. Collecting a sample of fly ash for use in laboratory testing.



Fig. A7. Collecting a sample in a thin-wall tube using a drive-tube hammer.



Fig. A8. Measuring water content and unit weight of SRPM after compaction.



Fig. A9. One of principal investigators (T. Edil) hard at work in the field.

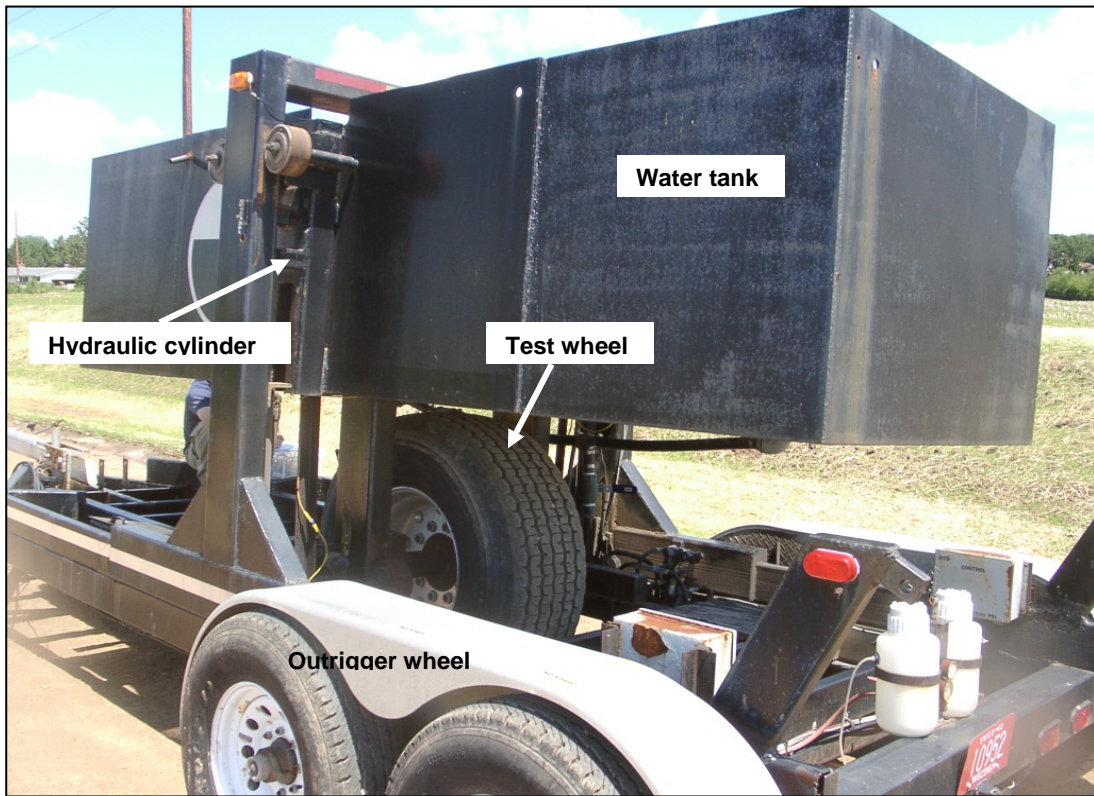


Fig. A10. RWD test apparatus.

APPENDIX B

**PHOTOGRAPHS OF
LYSIMETER CONSTRUCTION
AND
INSTALLATION OF INSTRUMENTS**



Fig. B1. Installing geomembrane for lysimeter.



Fig. B2. Installing collection tank for lysimeter.



Fig. B3. Installing water content reflectometer in subgrade.

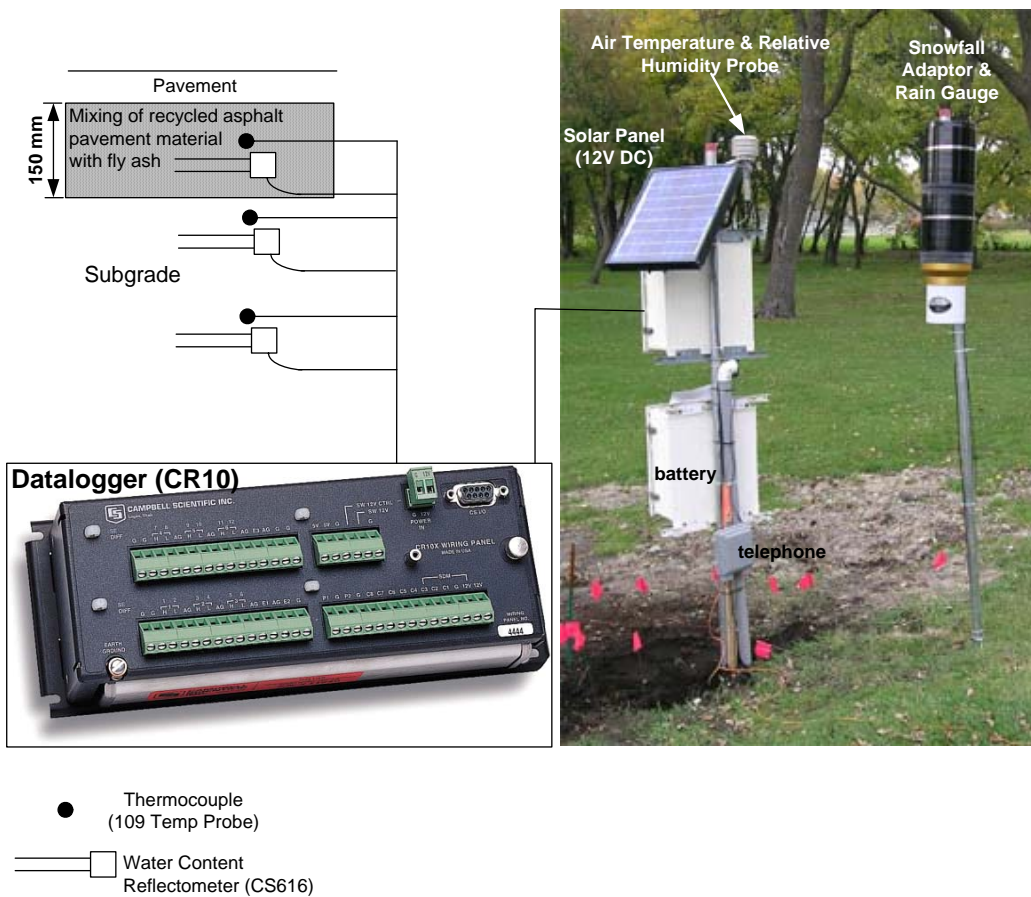


Fig. B4. Layout of field instrumentation.

APPENDIX C
LYSIMETER MONITORING DATA

Table C1. Summary of lysimeter data (except concentrations).

LYSIMETER DATA		16 m ²		Dry Density =	17.90	kN/m ³	Porosity =		0.31 <th colspan="2">L</th> <th colspan="4"></th>	L					
Site: Waseca, MN				Water Content =	8.00	%	PV =		747.5						
Lysimeter Size:				Depth =	0.15	m									
				Pump Volume Meter (g)											
Date	Sample ID	pH field	pH lab	Eh (mv)	EC (us/cm)	Comments	Weather	Air Temp	Start (gall)	End (gall)	Vol (L)	Cum Vol (L)	PVF	Drain (mm/d)	Comments
9/11/2004	-	-	-			start			0	0	0	0	0.00		
12/17/2004	-	-	-			no water	Sunny	1/9/1900	39.1	39.1	0	0.0	0.00	0.00	
4/5/2005	-	-	-			no water	-	-	0	0	0	0.0	0.00	0.00	
6/7/2005	W-06-07-05-	7.3	6.7	196		first water	-	-	400	477.5	290.6	290.6	0.39	0.29	
7/7/2005	W-07-07-05-	7.5	6.16	144.2			cloudy	65	477.5	593.5	435.0	725.6	0.97	0.91	
8/2/2005	W-08-02-05-	6.9	6.2	110.7			clear		594.5	712	440.6	1166.3	1.56	1.06	
8/23/2005	W-08-23-05-	7.1					clear	55	712	749.5	140.6	1306.9	1.75	0.42	
9/21/2005	W-09-21-05-	7.3	6.9	47.8	477		clear	70	749.5	760.1	39.8	1346.6	1.80	0.09	
10/6/2005	No analysis						cold	40	760.1	761.4	4.875	1351.5	1.81	0.02	
11/6/2005	No analysis						-	-	761.4	761.4	0	1351.5	1.81	0.00	Tank empty
12/29/2005	No analysis						-	-			0	1351.5	1.81	0.00	Tank empty
2/6/2006	No analysis						-	-			0	1351.5	1.81	0.00	Ice in Tank
3/23/2006	No analysis						-	-			0	1351.5	1.81	0.00	Tank empty
5/1/2006	W-05-01-06	7				water	clear	-	761.4	788.8	102.75	1454.3	1.95	0.16	

Table C2. Summary of concentrations in drainage from lysimeter.

Sample ID	PVF	Be ppb	B ppb	Ca ppb	Tl ppb	V ppb	Cr ppb
W-07-07-05	0.97	< 0.1	43.57	47927	< 0.02	1.45	2.46
W-08-02-05	1.56	<0.06	20.06	35737	< 0.02	0.47	3.02
W-08-23-05	1.75	<0.06	30.32	53000	<0.02	0.74	0.75
W-09-21-05	1.80	<0.06	39.4	61253	0.03	2.11	2.26
Sample ID	Mn ppb	Co ppb	Ni ppb	Cu ppb	Zn ppb	As ppb	Se ppb
W-07-07-05	1414	3.84	11.83	5.70	31.23	1.36	<2
W-08-02-05	1645	4.53	13.21	4.00	25.16	0.88	<2
W-08-23-05	2200	2.94	11.76	4.04	19.77	1.32	<2
W-09-21-05	1365	1.89	20.8	7.96	15.7	1.74	<2
Sample ID	Se ppb	Sr ppb	Mo ppb	Ag ppb	Cd ppb	Sn ppb	Sb ppb
W-07-07-05	<2	60.90	4.28	< 0.1	1.58	0.13	0.41
W-08-02-05	<2	53.13	0.47	<0.02	0.34	0.15	0.17
W-08-23-05	<2	74.97	0.55	<0.02	0.45	0.068	0.31
W-09-21-05	<2	102	0.50	<0.02	0.81	0.08	0.18
Sample ID	Ba ppb	Hg ppb	Pb ppb				
W-07-07-05	37.44	< 1	0.29				
W-08-02-05	49.64	< 0.2	0.54				
W-08-23-05	66.45	<0.2	0.92				
W-09-21-05	65.6	<0.2	1.01				

APPENDIX D

COLUMN LEACH TEST DATA

Table D1. Summary of concentrations in effluent from CLT on SRPM.

Concentrations from CLT on Waseca SRPM. All in units of µg/L

PVF	pH	Be	B	Ca	Tl	V	Cr	Mn	Co	Ni	Cu	Zn
0.5254	7.6	0.10	169	66922	0.03	10.30	7.70	19.8	1.84	29.0	121.0	802.8
0.7908	7.3	0.31	2196	160461	0.04	42.66	51.22	17.3	5.18	39.5	73.4	134.7
1.1285	7.5	0.28	2082	291257	0.06	29.46	4.40	317.2	5.76	41.5	46.1	20.8
1.5203	7.5	0.24	1694	300247	0.10	23.58	0.94	477.7	5.03	54.7	26.9	5.2
1.9905	7.3	0.30	1783	296740	0.10	23.19	0.90	426.6	4.65	48.8	19.5	14.2
3.1969	7.5	0.20	1259	188079	0.07	29.47	2.45	32.7	2.51	31.2	11.6	2.8
5.5932	7.3	0.17	1239	231	0.09	12.70	0.33	4.8	2.66	9.1	9.7	40.7
6.5471	7.8	0.19	1355	224460	0.05	13.40	0.25	184.6	2.03	23.0	8.9	4.5
Detection Limits:		0.100	0.200	5.000	0.006	0.060	0.040	0.030	0.010	0.050	0.070	0.200
PVF	As	Se	Sr	Mo	Ag	Cd	Sn	Sb	Ba	Hg	Pb	
0.5254	1.34	3.1	269	22.5	0.10	0.80	0.10	0.32	48.4	0.2	5.69	
0.7908	7.21	53.5	2159	89.8	0.17	3.41	0.11	3.06	136.7	0.2	7.94	
1.1285	7.08	59.8	3856	88.5	0.54	2.03	0.28	5.97	166.2	0.2	0.66	
1.5203	5.20	37.5	3963	80.8	0.22	2.79	0.12	8.30	159.2	0.2	0.67	
1.9905	4.59	27.1	4023	85.3	0.27	2.99	0.11	9.14	227.8	0.2	0.85	
3.1969	3.13	15.7	2807	54.5	0.21	3.39	0.12	10.64	344.2	0.2	0.57	
5.5932	6.1	19.0	3211	106.0	0.18	4.48	0.31	14.00	381.0	0.2	19.00	
6.5471	3.91	13.4	3186	139.3	0.19	4.31	0.08	11.20	382.9	0.2	4.97	
Detection Limits:		0.100	2.000	0.010	0.080	0.020	0.080	0.040	0.020	0.020	0.200	0.010

APPENDIX E
RESILIENT MODULUS CURVES FOR SRPM

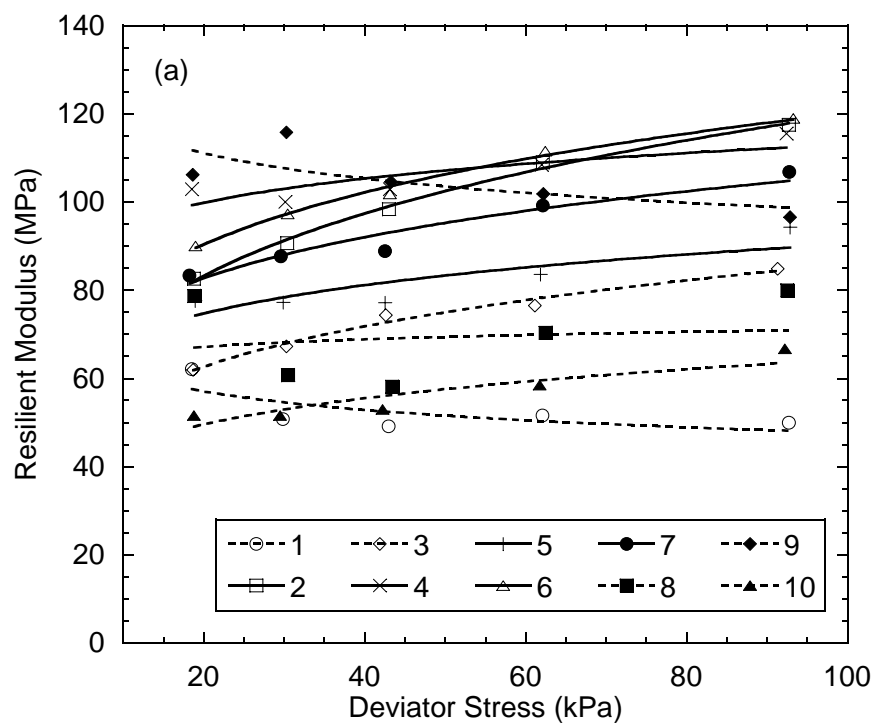


Fig. E1. Resilient modulus curves for SRPM.

APPENDIX F

ON-SITE METEOROLOGICAL DATA

(to be added in final copy....this is a big file)